An Incremental State Space Modelling Method of Power Systems Based on Measured Components Impedance Matrices in Local dq Frames

Zhou, Weihua; Wang, Yanbo; Chen, Zhe

Published in:
Proceedings of CIGRE Symposium Aalborg 2019

Publication date:
2019

Document Version
Accepted author manuscript, peer reviewed version

Symposium Aalborg, Denmark
4th-7th June 2019

041 (YM)

An Incremental State Space Modelling Method of Power Systems Based on Measured Components Impedance Matrices in Local dq Frames

W.H. ZHOU, Y.B. WANG, Z. CHEN
The Department of Energy Technology, Aalborg University
Denmark

SUMMARY

State space model (SSM)-based eigenvalues analysis method has been widely used to analyze stability issue of power electronics-dominated power systems. One important advantage of it is to perform participation factor analysis, so oscillation source can be identified. However, the derivation procedure of SSM is complicated for large-scale power systems. Furthermore, it's not easy to obtain system SSM due to unknown internal structure and parameters. This paper presents an incremental state space modelling method of power electronics-fed power system based on measured components impedance matrices on local dq frames. Terminal impedance frequency responses of all components are first measured by frequency scanning method on local dq frames. Then, SSMs of all components are fitted according to the measured dq impedance matrices by matrix fitting algorithm. Finally, SSM series operator and parallel operator are used to aggregate the fitted components SSMs in a recursive way. Simulation results show that the proposed incremental state space modelling method needs not know components internal information. In addition, dynamics of all components can be preserved in the established system SSM, while the information is lost in the existing dq impedance matrices aggregation method. The proposed incremental state space modelling method is also applicable for both mirror frequency decoupled system and mirror frequency coupled system.

KEYWORDS

DQ impedance matrix, impedance aggregation, matrix fitting algorithm, stability analysis, state space model operator.

wez@et.aau.dk.

INTRODUCTION

Renewable energies such as wind power and solar power are increasingly penetrating into power systems in recent years. Voltage source converters (VSCs) as an important interface are commonly used to transmit power energy into utility grid. However, oscillation phenomena during different frequency ranges have ben frequently reported in grid-connected VSCs.

State space model (SSM) has been widely used to analyze stability issue and identify oscillation source by participation analysis [1–3]. However, complicated mathematical derivation of SSM decreases analysis efficiency in large-scale power systems due to heavy computational burdens of high-dimensional matrices. To reduce computational burdens of SSM, modular state space modelling method has been originally proposed in [3,4], where the overall system is partitioned into different subsystems, and SSMs of subsystems are independently established. Then, system SSM is formulated by combining subsystems SSMs according to connection matrices among these subsystems. However, it's not practical to obtain detailed structure and parameters of all subsystems. System identification methods such as vector fitting (VF) algorithm and matrix fitting (MF) algorithm have been proposed to fit a SSM from a set of frequency responses [5,6]. However, a SSM cannot be fitted for an unstable power system in [5]. In addition, problematic components cannot be identified, since the whole system is regarded as a black box. Alternatively, [6] overcomes the two drawbacks by partitioning overall system into several stable subsystems of which the SSMs are fitted by VF algorithm, and system SSM is obtained by the aforementioned modular state space modelling method. However, PLL dynamics is ignored, which causes inaccurate impedance frequency characteristics in low-frequency range. In addition, topological characteristics of transmission network is not considered, which complicates modular state space modelling method.

The VF-based modular state space modelling method in [6] is developed in this paper by considering PLL dynamics and transmission network. In this work, dq impedance matrix is adopted. Different from phase-domain impedance, dq-domain impedance matrix is dependent on selection of dq reference frame, which means that the fitted SSM is related with dq reference frame. Commonly, dq-domain impedance matrix of a VSC is aligned with its terminal voltage. Therefore, established SSMs of subsystems in different dq frames should be transferred into the same dq frame, and all of these SSMs are combined together. Components impedance matrices aggregation in different dq frames have been widely studied in [7–11]. Rotation matrix is integrated into the VSC impedance model by a case specific method in [7]. However, the method is not applicable for an arbitrarily given network. In addition, the resulting source and load subsystem impedance matrices are complicated for larger-scale system. In [8, 9], a simpler method in which the alignment is achieved by a rotation matrix based on power flow information is proposed so that no internal information is needed. However, only local stability analysis results can be obtained, and instability sources cannot be identified. In addition, the impedance network modelling method proposed in [10, 11] fails to identify oscillation sources, since the whole power system is represented by an aggregated impedance matrix in the global dq frame. However, the combination of SSMs of different components in different dq frames has been slightly concerned.

Therefore, this paper proposes an incremental state space modelling method to integrate individual SSMs of different components extracted from terminal impedance frequency responses on local dq frames. SSMs of all components are first extracted from terminal frequency re-

sponses on local dq frames by MF algorithm. The SSM series operator and parallel operator are proposed in this paper to formulate SSM of overall system in a recursive way. The main contributions of this paper can be explained as follows. A MF algorithm-based modular state space modelling method is first proposed, where only terminal impedance frequency responses are required. Then, SSM series and parallel operators are proposed to combine small-signal dynamics of all components in a convenient way.

PROBLEM FORMULATION AND METHODOLOGY

In this section, the problem to be addressed in this work is first explained, followed by introducing one existing solution. And, the basis of methodology applied in this paper including VF and MF algorithms is introduced.

Problem formulation

Fig. 1 shows control diagram of a L-filtered VSC, where current control loop is used to track current reference i^*_{tdq}, and PLL is used to track phase angle of terminal voltage v_{tabc}. To analyze stability issue of VSC in low-frequency range, PLL dynamics is considered. Due to asymmetric impact of PLL on terminal impedance, 2×2 impedance matrix in dq frame shown as (1) should be used. The dq impedance matrix $\mathbf{Z}_{dq}$ is aligned to its terminal voltage v_{tabc}.

$$\mathbf{Z}_{dq} = (\mathbf{Z}_{out}^{-1} + \mathbf{G}_{id}\mathbf{G}_{del}((-\mathbf{G}_{ci}+\mathbf{G}_{dei})\mathbf{G}_{PLL}^{i} + \mathbf{G}_{PLL}^{d})\mathbf{K})^{-1} \cdot (\mathbf{I} + \mathbf{G}_{id}\mathbf{G}_{del}(\mathbf{G}_{ci}-\mathbf{G}_{dei})\mathbf{K}) \quad (1)$$

where bold letters indicate 2×2 matrices; $\mathbf{G}_{PLL}^{i}$, $\mathbf{G}_{PLL}^{d}$ are two asymmetric matrices related to PLL. Detailed derivation process and expression of each transfer function matrix can be found in [14].

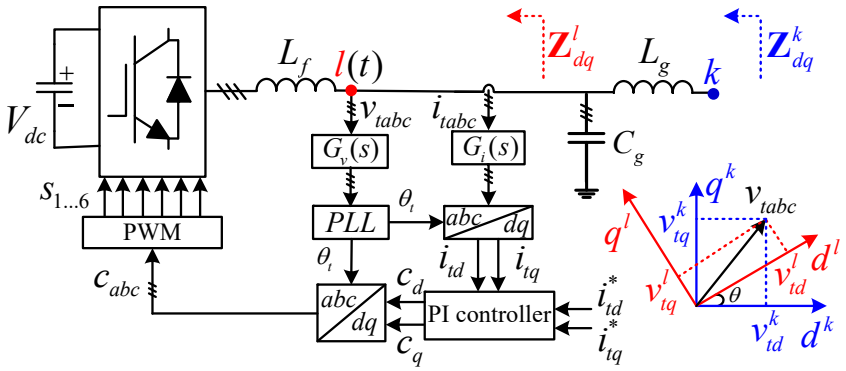

Figure 1. The control diagram of a L-filtered VSC with current control loop and PLL.

Fig. 1 shows control diagram of a VSC connected into capacitive grid, $\mathbf{Z}_{dq}$ should be transferred from l reference frame to k reference frame. The dq impedance matrix of the VSC in the two reference frames can be linked by (2) [7].

$$\mathbf{Z}^k_{dq} = \mathbf{R}_{dq}(\theta)\mathbf{Z}^l_{dq}\mathbf{R}^{-1}_{dq}(\theta) \quad (2)$$

where $\mathbf{R}_{dq}(\theta) = [\cos\theta, \sin\theta; -\sin\theta, \cos\theta]$ is rotation matrix, and θ is angle difference of voltages between node l and node k as shown in Fig. 1.

One existing solution to align local dq frames and aggregate dq impedance matrices

Two cases including both series connection and parallel connection situations where two components are not limited to VSCs are given in Fig. 2. Impedance series operator $\oplus'$ and impedance parallel operator $\odot'$ are defined.

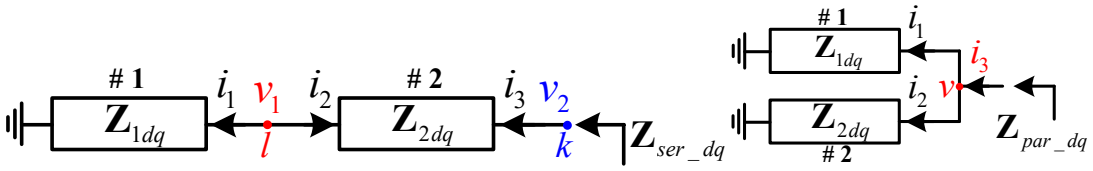

Figure 2. Two basic components connection cases. (a) Series connection case; (b) Parallel connection case.

- **Impedance series operator:** $\mathbf{Z}_{1dq}$ should be first rotated from l reference point to k reference point to perform circuit series principle. The total series impedance $\mathbf{Z}_{ser\_dq}$ is given as (3).

$$\mathbf{Z}_{ser\_dq} = \mathbf{Z}^k_{1dq} + \mathbf{Z}^k_{2dq} = \mathbf{R}_{dq}(\theta)\mathbf{Z}_{1dq}\mathbf{R}^{-1}_{dq}(\theta) + \mathbf{Z}_{2dq} = \mathbf{Z}_{1dq} \oplus' \mathbf{Z}_{2dq} \tag{3}$$

  where $\mathbf{Z}^k_{1dq}$ and $\mathbf{Z}^k_{2dq}$ are two dq impedance matrices based on k reference point, while $\mathbf{Z}_{1dq}$ and $\mathbf{Z}_{2dq}$ are two dq impedance matrices based on their own terminal reference points. The definition of $\mathbf{R}_{dq}(\theta)$ is the same as that in (2). Impedance series operator $\oplus'$ is also defined in (3).

  If component #1 is mirror frequency decoupled (MFD) (i.e., $Z_{1dd} = Z_{1qq}$, $Z_{1dq} = -Z_{1qd}$), e.g., passive RLC elements, impedance matrix rotation invariance characteristics is satisfied [8], which is given as (4).

$$\mathbf{Z}^k_{1dq} = \mathbf{R}_{dq}(\theta)\mathbf{Z}_{1dq}\mathbf{R}^{-1}_{dq}(\theta) = \mathbf{Z}_{1dq} \tag{4}$$

  (4) means that dq impedance matrix of passive RLC elements is independent on selection of dq frame.
- **Impedance parallel operator:** Different from series connection case, terminal voltages of the two components #1 and #2 are the same for parallel connection case, which means that no matrix rotation operation is required. The total parallel impedance $\mathbf{Z}_{par\_dq}$ can be calculated by the basic circuit theory, which is given as (5).

$$\mathbf{Z}_{par\_dq} = \mathbf{Z}_{1dq} \odot' \mathbf{Z}_{2dq} = \frac{\mathbf{Z}_{1dq}\mathbf{Z}_{2dq}}{\mathbf{Z}_{1dq} + \mathbf{Z}_{2dq}} \tag{5}$$

Based on the two basic operators, the aggregated impedance matrix of larger-scale power system can be calculated in a recursive way. However, it can be seen that the dynamics of all components are merged, so that instability sources cannot be identified.

Basis of VF and MF

VF and MF algorithms are originally proposed in [12, 13]. VF can generate a rational model on pole-residue form (6) for a series of discrete frequency responses of a single-input single-output (SISO) system.

$$f(s) = \frac{r_m}{s - p_m} + \frac{r_{m-1}}{s - p_{m-1}} \ldots + \frac{r_1}{s - p_1} + D + sE = \mathbf{C}(s\mathbf{I} - \mathbf{A})^{-1}\mathbf{B} + D + sE \tag{6}$$

where $(r_i, p_i)(i = 1, 2..., m)$ is the ith residue-pole pair. D is the direct through component, and E is zero if $f(s)$ is proper. $\mathbf{A} = diag(p_1, p_2, ...p_m)$, $\mathbf{B} = [1, 1, ...1]_m{}^T$, $\mathbf{C} = [r_1, r_2, ...r_m]$. Thus, $f(s)$ can be represented in form of SSM (7).

$$\begin{aligned} \dot{x} &= \mathbf{A}x + \mathbf{B}u \\ y &= \mathbf{C}x + Du + sE \end{aligned} \tag{7}$$

MF can generate a rational model on pole-residue form for a series of discrete frequency responses of a multiple-input and multiple-output (MIMO) system. Taking a k-port MIMO system as an example, the fitted transfer function matrix is given as (8).

$$\mathbf{F(s)} = \frac{\mathbf{R}_m}{s - p_m} + \frac{\mathbf{R}_{m-1}}{s - p_{m-1}} ... + \frac{\mathbf{R}_1}{s - p_1} + \mathbf{D} + s\mathbf{E} = \mathbf{C}(s\mathbf{I} - \mathbf{A})^{-1}\mathbf{B} + \mathbf{D} + s\mathbf{E} \tag{8}$$

where $\mathbf{A} = diag(diag(p_1, p_2...p_m), ..., diag(p_1, p_2...p_m))_k$, $\mathbf{B} = diag([1, 1, ...1]_m{}^T, ..., diag[1, 1, ...1]_m{}^T)_k$, $\mathbf{C} = [\mathbf{R}_1(:,1), \mathbf{R}_2(:,1)..., \mathbf{R}_m(:,1), \mathbf{R}_1(:,2), \mathbf{R}_2(:,2)..., \mathbf{R}_m(:,2), ..., \mathbf{R}_1(:,k), \mathbf{R}_2(:,k)..., \mathbf{R}_m(:,k)]$. It can be seen from (8) that all elements in $\mathbf{F}(s)$ share the same poles sets $(p_1, p_2..., p_m)$ which can be used to assess stability issue of the MIMO system.

PROPOSED INCREMENTAL STATE SPACE MODELLING METHOD

Although the dq impedance matrices aggregation method in (3) and (5) can be used to implement impedance-based stability analysis, individual component dynamics is lost in the aggregation procedure. The combination of SSM of different components can maintain individual component dynamics in the finally-established system SSM, so contribution of each component to instability phenomena can be calculated. In this section, definition of the proposed SSM series operator $\oplus$ and parallel operator $\odot$ is first explained, and details of the proposed incremental state space modelling method are given.

Definition of proposed SSM series operator $\oplus$ and parallel operator $\odot$

- **Proposed SSM series operator $\oplus$:** Series connection case shown in Fig. 2(a) is used to explain the proposed SSM series operator $\oplus$. Similar with dq frames alignment for dq impedance matrices aggregation, the established two SSMs of components #1 and #2 on local dq frames are first aligned. SSMs of component #1 based on l reference point and k reference point are assumed as (9) and (10).

$$\begin{aligned} \dot{x} &= \mathbf{A}_l x + \mathbf{B}_l i_1 \\ v_1 &= \mathbf{C}_l x + D_l i_1 + sE_l \end{aligned} \tag{9}$$

$$\begin{aligned} \dot{x} &= \mathbf{A}_k x + \mathbf{B}_k i_1 \\ v_1 &= \mathbf{C}_k x + D_k i_1 + sE_k \end{aligned} \tag{10}$$

The relationship between SSM matrices in the two dq frames is given as (11) by combining (3), (6) and (7).

$$\begin{aligned} &\mathbf{Z}^k_{1dq} = \frac{v^k_{1dq}}{i^k_{1dq}} = \mathbf{R}_{dq}(\theta)\mathbf{Z}^l_{1dq}\mathbf{R}^{-1}_{dq}(\theta) = \mathbf{R}_{dq}(\theta)\frac{v^l_{1dq}}{i^l_{1dq}}\mathbf{R}^{-1}_{dq}(\theta) \\ &\mathbf{C}_k(sI - \mathbf{A}_k)^{-1}\mathbf{B}_k + D_k + sE_k = \mathbf{R}_{dq}(\theta)(\mathbf{C}_l(sI - \mathbf{A}_l)^{-1}\mathbf{B}_l + D_l + sE_l)\mathbf{R}^{-1}_{dq}(\theta) \end{aligned} \tag{11}$$

It can be seen from (11) that the SSM of component #1 based on k reference point can be calculated once the SSM based on l reference point and angle difference of voltages

of node k and node l are known. Similar with (4), if component #1 is MFD, e.g., passive RLC elements, rotation invariance characteristics is also applicable.

Then, SSMs of components #1 and #2 are assumed to have been derived in the same reference frame k as (12) and (13).

$$\begin{aligned} \dot{x}_1 &= \mathbf{A}_1 x_1 + \mathbf{B}_1 u_1 \\ y_1 &= \mathbf{C}_1 x_1 + D_1 u_1 \end{aligned} \tag{12}$$

$$\begin{aligned} \dot{x}_2 &= \mathbf{A}_2 x_2 + \mathbf{B}_2 u_2 \\ y_2 &= \mathbf{C}_2 x_2 + \mathbf{D}_2 u_2 \end{aligned} \tag{13}$$

where $u_1 = v_1$, $y_1 = i_1$, $u_2 = [i_2, i_3]^T$, $y_2 = [v_1, v_2]^T$, $i_2 = -i_1$. Then, these SSM elements can be combined together, i.e., $\mathbf{A} = diag(\mathbf{A}_1, \mathbf{A}_2)$, $\mathbf{B} = diag(\mathbf{B}_1, \mathbf{B}_2)$, $\mathbf{C} = diag(\mathbf{C}_1, \mathbf{C}_2)$, $\mathbf{D} = diag(\mathbf{D}_1, \mathbf{D}_2)$, $x = [x_1, x_2]^T$, $u = [u_1, u_2]^T$, $y = [y_1, y_2]^T$. Thus, components input u and output y are linked with system input $a = i_3$ and output $b = v_2$ as (14).

$$\begin{aligned} u &= \mathbf{L}_1 y + \mathbf{L}_2 a \\ b &= \mathbf{L}_3 y + \mathbf{L}_4 a \end{aligned} \tag{14}$$

Where $\mathbf{L}_1 = [0, 1; -1, 0]$, $\mathbf{L}_2 = 0$, $\mathbf{L}_3 = [0, 1]$ and $\mathbf{L}_4 = 0$. System SSM can be derived as (15).

$$\begin{aligned} \dot{x} &= \mathbf{F} x + \mathbf{G} a \\ b &= \mathbf{H} x + \mathbf{J} a \end{aligned} \tag{15}$$

where $\mathbf{F} = \mathbf{A} + \mathbf{B}\mathbf{L}_1(\mathbf{I} - \mathbf{D}\mathbf{L}_1)^{-1}\mathbf{C}$, $\mathbf{G} = \mathbf{B}\mathbf{L}_1(\mathbf{I} - \mathbf{D}\mathbf{L}_1)^{-1}\mathbf{D}\mathbf{L}_2 + \mathbf{B}\mathbf{L}_2$, $\mathbf{H} = \mathbf{L}_3(\mathbf{I} - \mathbf{D}\mathbf{L}_1)^{-1}\mathbf{C}$, $\mathbf{J} = \mathbf{L}_3(\mathbf{I} - \mathbf{D}\mathbf{L}_1)^{-1}\mathbf{D}\mathbf{L}_2 + \mathbf{L}_4$. Generally, for a series-chain model which consists of a terminal part and multiple linkage parts (a terminal part is defined as a one-port network as # 1 in Fig. 2 (a), while a linkage part is defined as a two-port network as # 2 in Fig. 2 (a)), the proposed SSM series operator $\oplus$ is defined as (16) to combine all components SSMs.

$$S_T \oplus S_1 \oplus S_2 ... \oplus S_m = S_{ser} \tag{16}$$

where S_T, $S_{1,2...,m}$ and S_{ser} are the SSMs of the terminal part, m linkage parts and overall system in their own dq reference frames, respectively. They are in the forms of (12), (13) and (15), respectively. Associative law is met for the SSM series operator $\oplus$, shown as (17).

$$S_T \oplus S_1 \oplus S_2 ... \oplus S_p \oplus S_{p+1} ... \oplus S_m = S_T \oplus S_1 \oplus S_2 ... \oplus (S_p \oplus S_{p+1}) ... \oplus S_m \quad \forall p \in [1, m-1] \tag{17}$$

However, commutative law is not satisfied for the SSM series operator $\oplus$.

- **Proposed SSM parallel operator $\odot$:** Parallel connection case shown in Fig. 2(b) is used to explain the proposed SSM parallel operator. SSMs of components #1 and #2 are assumed to have been derived in the same reference frame aa shown in (12) and (13). The minor difference with series connection case is that $i_2 \neq -i_1$, system input $a = i_3 = i_1 + i_2$ and system output $b = v$. By solving (14), the matrices can be solved as $\mathbf{L}_1 = [0, -1; 1, 0]$, $\mathbf{L}_2 = [1; 0]$, $\mathbf{L}_3 = [1, 0]$ and $\mathbf{L}_4 = 0$. The representations of $\mathbf{F}$, $\mathbf{G}$, $\mathbf{H}$ and $\mathbf{J}$ are the same as series connection case. Similarly, the SSM parallel operator $\odot$ is proposed to combine the SSMs of multiple terminal parts S_{T1}, S_{T2}..., S_{Tm}, shown as (18).

$$S_{T1} \odot S_{T2} ... \odot S_{Tm} = S_{par} \tag{18}$$

where S_{T1}, S_{T2}..., S_{Tm} are in the form of (12) and S_{par} is in the form of (15). Both associative law and commutative law are satisfied for the SSM parallel operator $\odot$ as shown in (19).

$$S_{T1} \odot S_{T2} \ldots \odot S_{Tp} \odot S_{T(p+1)} \ldots \odot S_{Tm} = S_{T1} \odot S_{T2} \ldots \odot (S_{T(p+1)} \odot S_{Tp}) \ldots \odot S_{Tm} \quad \forall p \in [1, m-1] \tag{19}$$

Implementation procedure of proposed modelling method

Fig. 3 shows implementation procedure of the proposed incremental state space modelling method, which includes two steps.

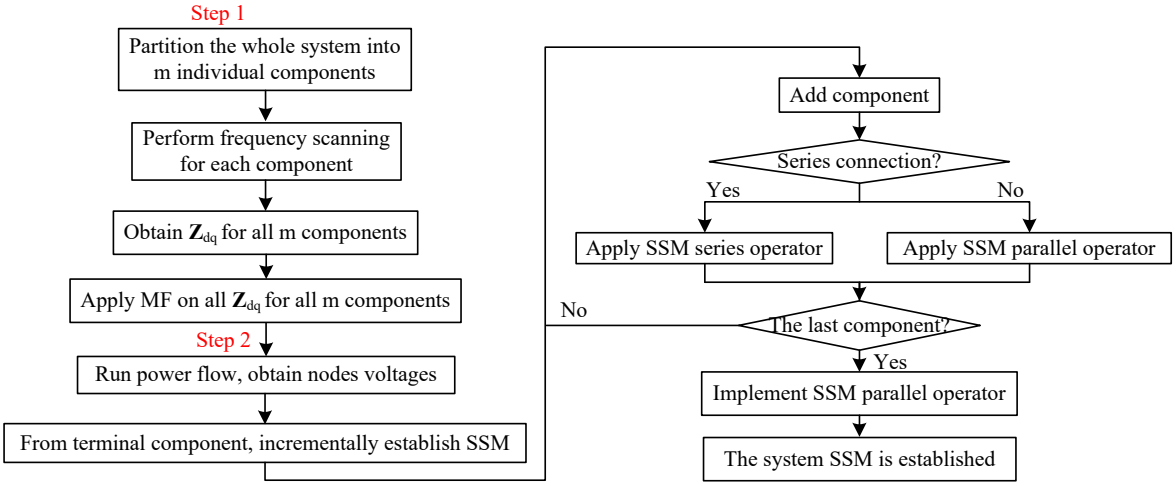

Figure 3. Flowchart of the proposed incremental state space modelling method.

- **The Step 1 is to extract individual SSMs from terminal impedance frequency responses on local dq frames by MF algorithm.** The overall system is first partitioned into m individual components. Then, frequency scanning is performed for each component. Discrete impedance frequency response of each component on local dq frame during concerned frequency range can be extracted. And, the SSM matrices in (8) can be generated by applying MF algorithm on these discrete impedance frequency responses.
- **The Step 2 is to establish SSM of the overall system using the proposed SSM operators $\oplus$ and $\odot$.** Simulation is first run to obtain all nodes voltages by power flow. Then, components are combined together by using proposed series and parallel operators in a recursive way. The last component is regarded as connected with the rest part in parallel, so the SSM parallel operator $\odot$ is used in the last step.

SIMULATION VERIFICATION

In this section, simulation is implemented to validate effectiveness of the proposed incremental state space modelling method by two cases. Figure. 4 shows diagrams of two cases, including passive RLC network and four VSCs-based power system.

Case 1: Passive RLC network

The proposed state space modelling method is first validated in a passive RLC network, where parameters of RLC components are given in Table 1. The dq impedance matrix $\mathbf{Z}_{idq}(i = 1, 2..., 10)$ and $\mathbf{Z}_g$ in their own dq reference frames can be obtained by implementing frequency

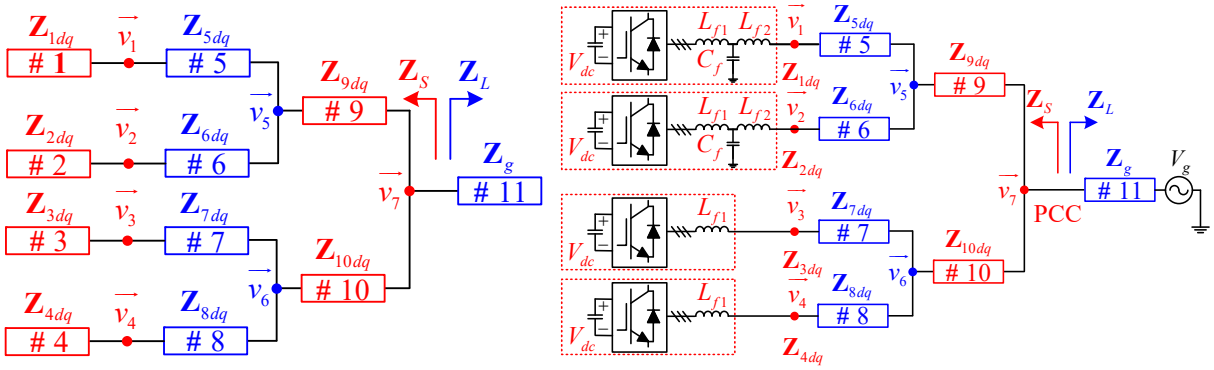

Figure 4. Two studied cases. (a) Passive RLC network; (b) Four VSCs-based power system.

scanning at PCCs, as shown in Fig. 3 (100 frequency points are logarithmically distributed in frequency range [1Hz, 5kHz]). Fig. 5 shows frequency characteristics of the aggregated dq impedance matrix $\mathbf{Z}_{S\_with\_rot}$, the aggregated dq impedance matrix $\mathbf{Z}_{S\_no\_rot}$ and measured frequency responses $\mathbf{Z}_{S\_mea}$. It can be seen from Fig. 5 that frequency characteristics of $\mathbf{Z}_{S\_with\_rot}$, $\mathbf{Z}_{S\_no\_rot}$ and $\mathbf{Z}_{S\_mea}$ are nearly matched, which thus validates effectiveness of the impedance series operator and impedance parallel operator. Also, it shows that dq impedance matrix of passive RLC elements are rotation invariant.

Table 1
COMPONENTS PARAMETERS OF THE PASSIVE RLC NETWORK.

Components	# 1	# 2	# 3	# 4	# 5	# 6
Resistances	0.0218Ω	0.0436Ω	0.1960Ω	0.2178Ω	0.0871Ω	0.1742Ω
Inductances	0.7mH	1.4mH	6.2mH	6.9mH	2.8mH	5.6mH
Components	# 7	# 8	# 9	# 10	# 11	
Resistances	0.1525Ω	0.1307Ω	0.0653Ω	0.1089Ω	0.0871Ω	
Inductances	4.9mH	4.2mH	2.1mH	3.5mH	2.8mH	

The dq impedance matrix of $\mathbf{Z}_L$ is also obtained by frequency scanning method. The measured impedance matrix is defined as $\mathbf{Z}_{L\_mea}$. In addition, measured system dq impedance matrix $\mathbf{Z}_{sys_mea}$is defined as $\mathbf{Z}_{L\_mea}//\mathbf{Z}_{S\_mea}$. Frequency responses of $\mathbf{Z}_{S\_mea}$, $\mathbf{Z}_{L\_mea}$ and $\mathbf{Z}_{sys\_mea}$ are given in Fig. 6.

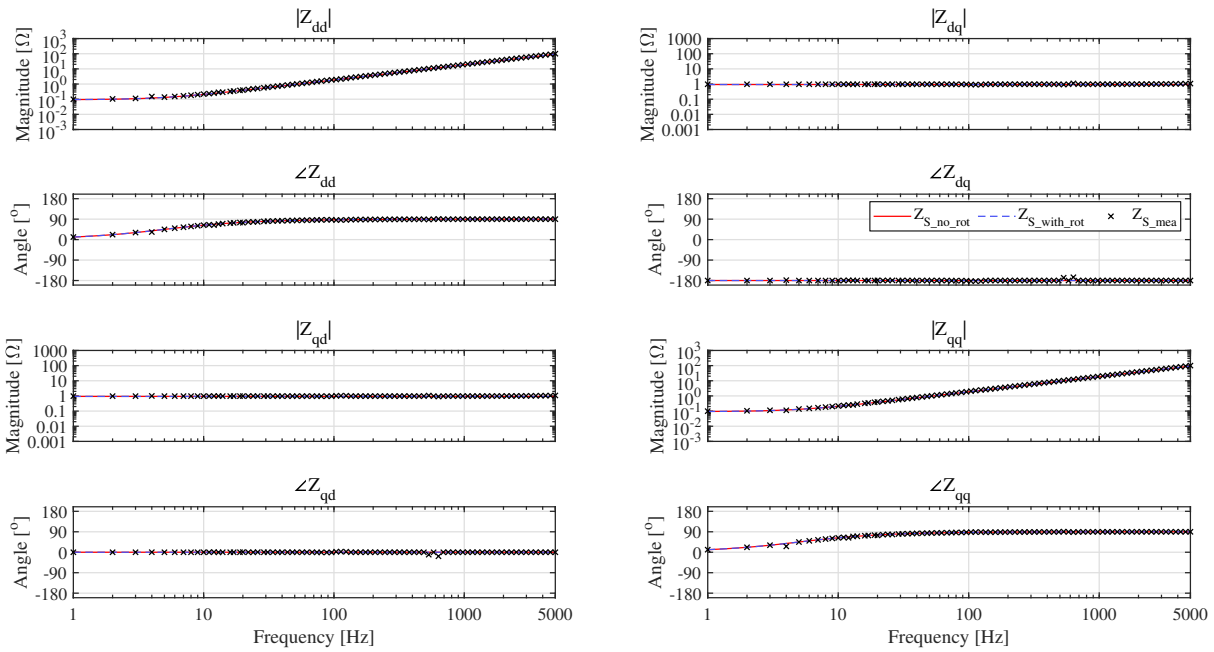

Figure 5. Verification of dq impedance matrix rotation invariance of passive RLC components ($\mathbf{Z}_{S\_no\_rot}$/$\mathbf{Z}_{S\_with\_rot}$ is the aggregated dq impedance matrix obtained without/with using rotation operation. $\mathbf{Z}_{S\_mea}$ is the dq impedance matrix obtained by directly performing frequency scanning at PCC).

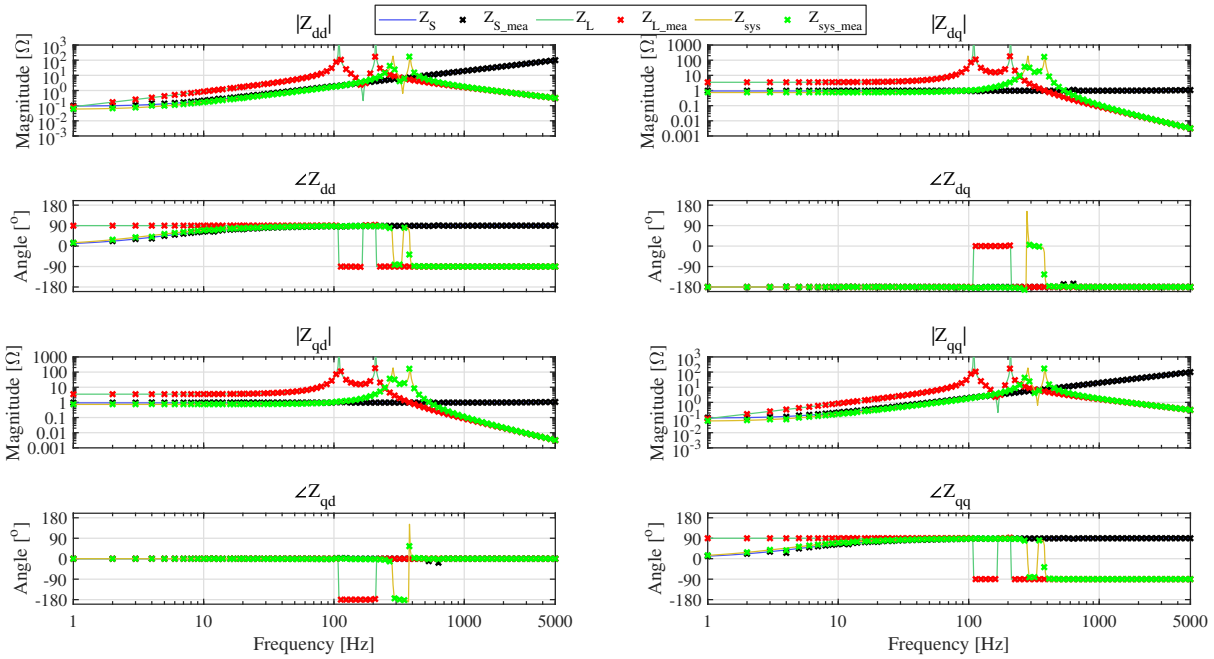

Figure 6. Bode diagrams of $\mathbf{Z}_{S\_mea}$, $\mathbf{Z}_{L\_mea}$ and $\mathbf{Z}_{sys\_mea}$ for case 1 ($\mathbf{Z}_{S\_mea}$/$\mathbf{Z}_{L\_mea}$ is the dq impedance matrix of source/load part obtained by directly performing frequency scanning at PCC. $\mathbf{Z}_{sys\_mea}$ is defined as $\mathbf{Z}_{S\_mea}$//$\mathbf{Z}_{L\_mea}$. $\mathbf{Z}_S$, $\mathbf{Z}_L$ and $\mathbf{Z}_{sys}$ are corresponding theoretically-derived curves).

Apparent impedance analysis method proposed in [5] is applied to extract system SSM from $\mathbf{Z}_{sys\_mea}$. Fig. 7 shows the fitted result with fitting order chosen as 4. It can be seen that the fitting result nearly matches the measured frequency responses.. The eigenvalues of the fitted system SSM are given in Fig. 8. It can be seen that two magnitude peaks at 268Hz and 379Hz in Fig. 7 are captured by the established SSM (i.e., $\frac{1745}{2\pi} = 277.7$Hz, $\frac{2373}{2\pi} = 377.7$Hz). In addition, the eigenvalues of the established system SSM obtained by the proposed incremental state space modelling method are also plotted in Fig. 8. It can be seen that, the proposed state

space modelling method can achieve almost the same eigenvalues as the state space modelling method proposed in [5]. The advantage of the proposed state space modelling method lies in that the contribution of each component to each eigenvalue can be calculated quantitatively, which is not impossible in both existing dq impedance matrix aggregation method [7–11] and apparent impedance analysis method [5].

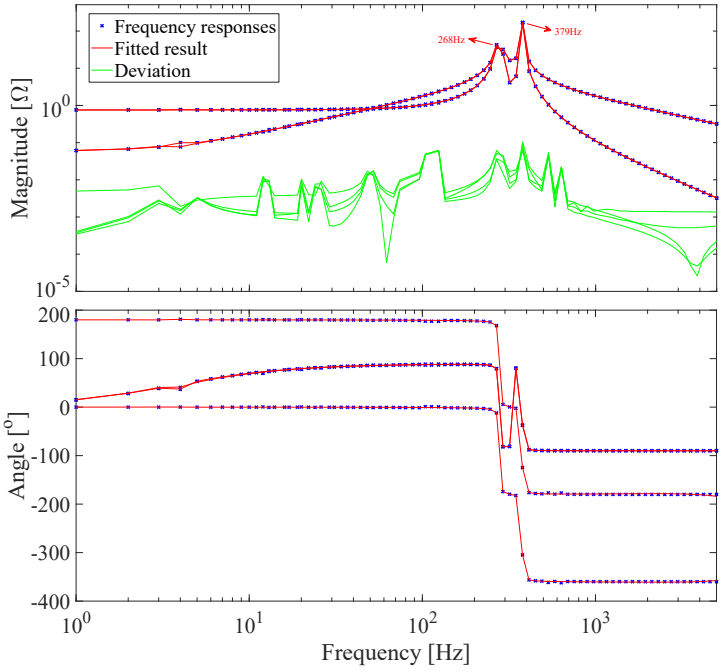

Figure 7. MF result of $\mathbf{Z}_{sys\_mea}$ for case 1.

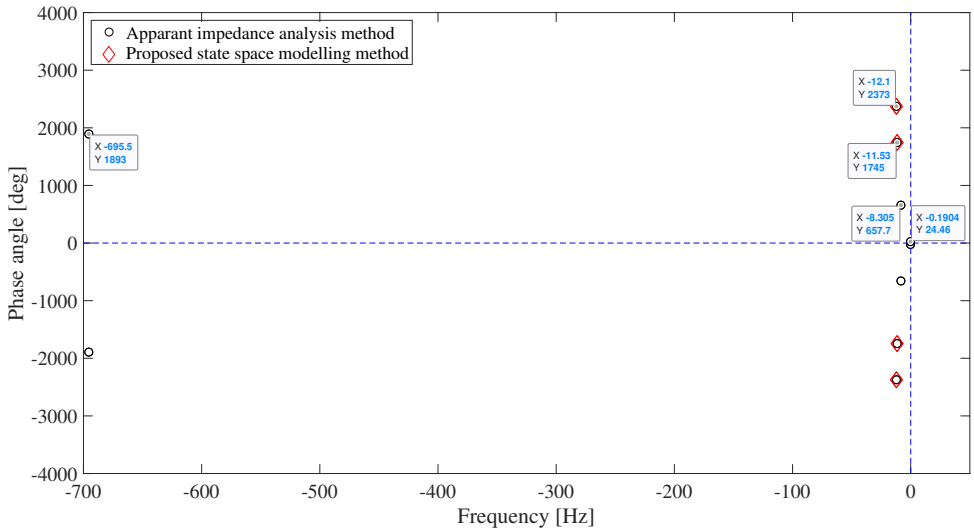

Figure 8. System eigenvalues for case 1 obtained by the apparent impedance analysis method proposed in [5] and the incremental state space modelling method proposed in this paper.

Case 2: Four VSCs-based power systems with RLC elements

In case 2, four terminal RLC components #1, #2, #3 and #4 are replaced by four VSCs under the control structure shown in Fig. 1. Specifically, VSCs #1 and #2 are with LCL filters, and VSCs #3 and #4 are with L filters, respectively. Circuit and control parameters of VSCs #3 and #4 are referred from [8], and are listed in Table 2. In addition, grid side filter inductor L_{f2} and

Table 2
CIRCUIT AND CONTROL PARAMETERS OF FOUR VSCS.

Parameters	Values	Parameters	Values
dc-link voltage V_{dc}	1150V	Grid voltage V_g (Phase-phase Vrms)	690V
Grid fundamental frequency	50Hz	Sampling/Switching frequency f_s/f_s'	10kHz
Inverter side filter inductor L_{f1}	6.93mH	Inverter side filter resistance R_{f1}	0.44Ω
Grid side filter inductor L_{f2}	6.93mH	Grid side filter resistance R_{f2}	0.44Ω
Filter capacitance C_f	10μF	Filter capacitor resistance R_{cf}	0.44Ω
Grid capacitance C_g	100μF	Grid inductance L_g	10mH
Current controller $K_{pi}(p.u./\mathrm{A})$	6.4×10^{-4}	Current controller $K_{ii}(p.u./(\mathrm{As}))$	0.161
PLL controller $K_{pPLL}(rad/(\mathrm{Vs}))$	7.58×10^{-3}	Current controller $K_{iPLL}(Vs^2)$	0.152

filter capacitor C_f are only used for VSCs #1 and #2.

A small voltage perturbation including 100 frequency points logarithmically distributed during frequency range from 1Hz to 5kHz is injected into PCC points to extract frequency responses. Fig. 9 shows frequency characteristics of the measured dq impedance matrix $\mathbf{Z}_{dq\_mea}$ and theoretically-derived dq impedance matrix $\mathbf{Z}_{dq\_the}$ using (1) for VSCs #1 and #2. Similarly, the measured and theoretically-derived results for VSCs #3 and #4 are shown in Fig. 10. It can be seen from Figs. 9 and 10 that dq impedance frequency characteristics for both LCL-type VSC and L-type VSC have been identified by frequency scanning method.

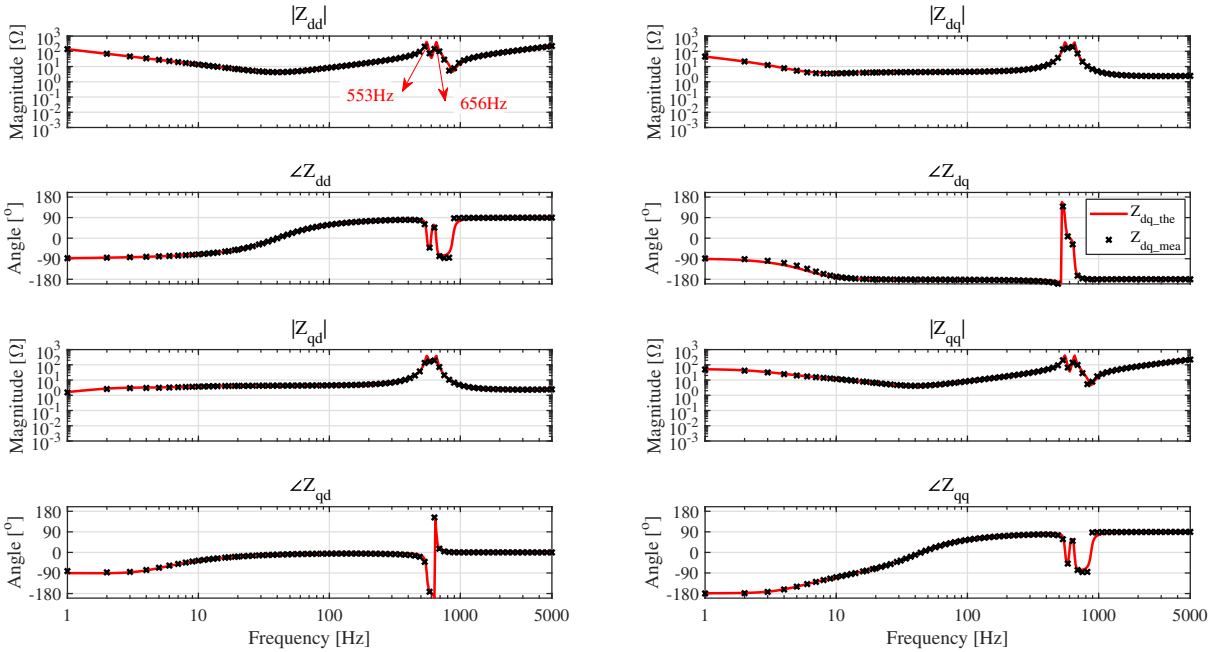

Figure 9. Bode diagrams of frequency scanning-based $\mathbf{Z}_{dq\_mea}$ and theoretically-derived $\mathbf{Z}_{dq\_the}$ of VSCs #1 and #2.

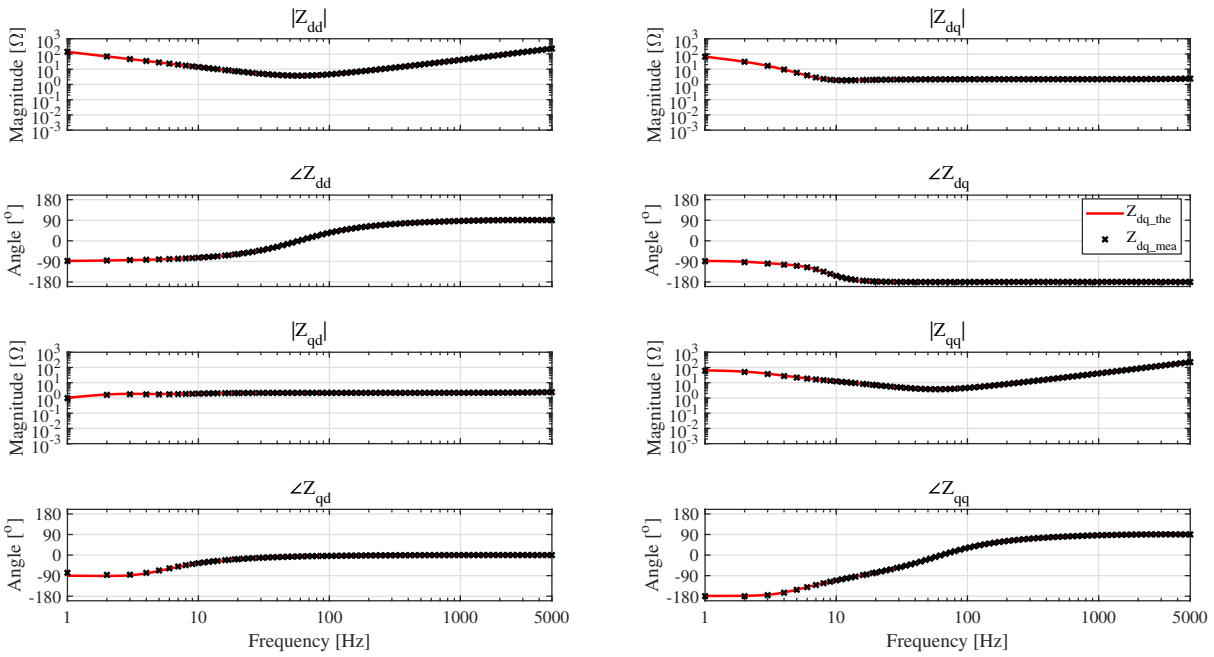

Figure 10. Bode diagrams of frequency scanning-based $\mathbf{Z}_{dq\_mea}$ and theoretically-derived $\mathbf{Z}_{dq\_the}$ of VSCs #3 and #4.

The measured impedance frequency responses for both kinds of VSCs are then fitted by MF algorithm. The eigenvalues of the fitted 10-order SSMs for four VSCs are listed in Table 3. As for VSCs #1 and #2, it can be seen from Fig. 9 and Table 3 that, the imaginary part of these extracted eigenvalues agree with the magnitude peaks of the impedance-frequency curves, i.e., 554.0661Hz is close to 553Hz, and 654.3337 Hz is close to 656Hz. As for VSCs #3 and #4, the fitted frequency 346.7350Hz has a high damping coefficient, which means that no magnitude peak will appear in its Bode diagram. It agrees with the Bode diagram shown in Fig. 10. These fitted SSMs of all VSCs will be used to establish system SSM by the proposed state space modelling method.

Table 3
EIGENVALUES OF THE FITTED 10-ORDER SSMS OF FOUR VSCS USING MF ALGORITHM.

VSCs #1 and #2	Frequency [Hz]	VSCs #3 and #4	Frequency [Hz]
-0.0031		-0.0135	
-33.8222		-3.1474	
-7.1911e+04		-12.8606	
-1.1576e+05		-30.5599	
-15.9002±11.4563i	1.8233	-14.4804 ±11.3011i	1.7986
-7.3817e+01 ± 3.4813e+03i	554.0661	-1.9357e+04 ± 2.1786e+03i	346.7350
-7.1833e+01 ± 4.1113e+03i	654.3337	-9.4684e+03 ± 1.3812e+05i	21982

In addition, $\mathbf{Z}_{S\_mea}$ and $\mathbf{Z}_{L\_mea}$ can be obtained by directly performing frequency scanning at PCC. The Bode diagrams of $\mathbf{Z}_{S\_mea}$ and $\mathbf{Z}_{L\_mea}$ are shown as the black and red crossed curves in Fig. 11. $\mathbf{Z}_{sys\_mea}$ is defined as $\mathbf{Z}_{S\_mea}$ // $\mathbf{Z}_{L\_mea}$, and the Bode diagram is shown as the green crossed curve in Fig. 11. It can be seen that the dq impedance matrix of both source and load parts can be obtained by frequency scanning method.

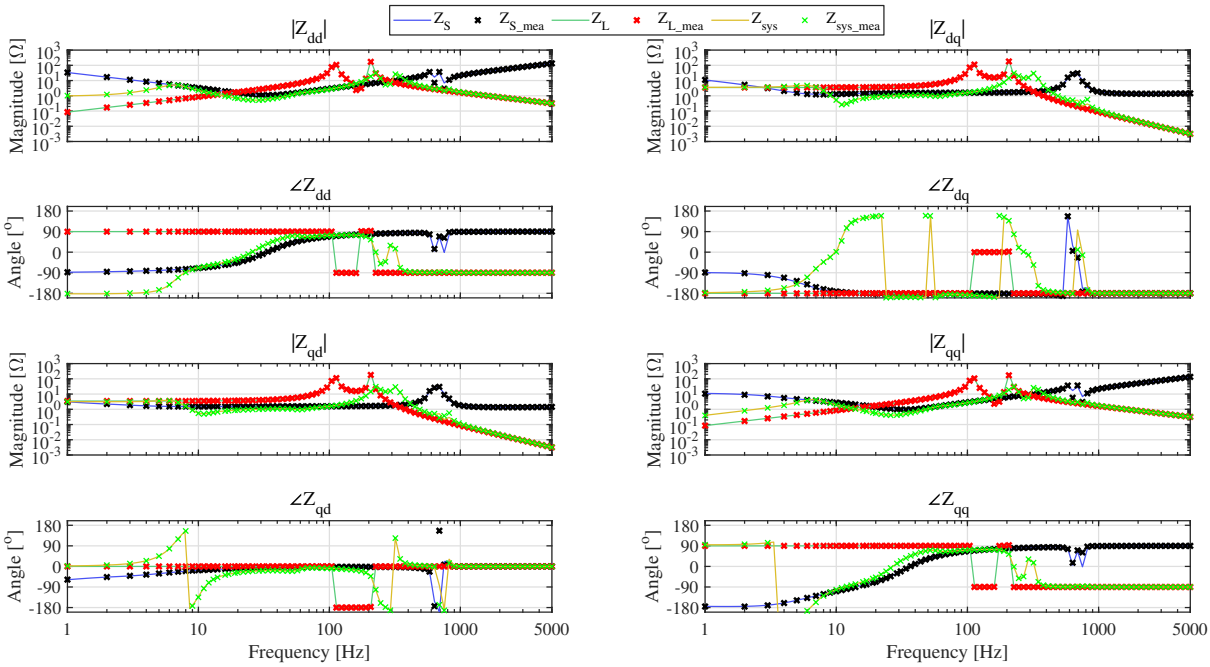

Figure 11. Bode diagrams of $\mathbf{Z}_{S\_mea}$, $\mathbf{Z}_{L\_mea}$ and $\mathbf{Z}_{sys\_mea}$ for case 2 obtained by directly performing frequency scanning at PCC ($\mathbf{Z}_{S\_mea}$/$\mathbf{Z}_{L\_mea}$ is the dq impedance matrix of source/load part obtained by directly performing frequency scanning at PCC. $\mathbf{Z}_{sys\_mea}$ is defined as $\mathbf{Z}_{S\_mea}$//$\mathbf{Z}_{L\_mea}$. $\mathbf{Z}_S$, $\mathbf{Z}_L$ and $\mathbf{Z}_{sys}$ are corresponding theoretically-derived curves).

MF algorithm can be used to extract system SSM from $\mathbf{Z}_{sys\_mea}$ by the method proposed in [5], and the eigenvalues of the established system SSM are plotted in Fig. 12. The eigenvalues of the established system SSM using the proposed method are also plotted in Fig. 12. It can be seen from Fig. 12 that, both system state space modelling methods obtain almost the same eigenvalues. In addition, these eigenvalues also agree with the magnitude peaks of $\mathbf{Z}_{sys\_mea}$. It shows that the proposed state space modelling method can obtain the same stability analysis conclusion as the impedance-based stability criterion and the apparent impedance analysis method. It should be noted that, compared with the other two methods, the system SSM derivation process using the method proposed in this paper can preserve individual components dynamics, thus PFs of all components can be calculated.

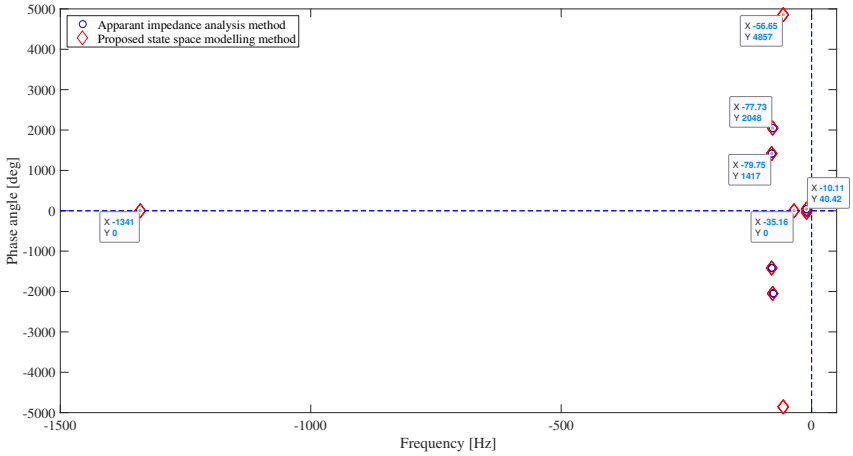

Figure 12. System eigenvalues for case 2 obtained by the "apparent impedance" analysis method proposed in [5] and the incremental state space modelling method proposed in this paper.

CONCLUSIONS

This paper presents an incremental state space modelling method of power systems based on measured components impedance matrices on local dq frames. SSMs of all components are first extracted from terminal impedance frequency responses on local dq frames by MF algorithm. Series operator and parallel operator are proposed to combine SSMs of different components in a recursive way. Simulation results show that the proposed state space modelling method can obtain the critical eigenvalues for stability analysis. Compared with the existing dq impedance matrices aggregation method, the proposed method can maintain individual dynamics by using the proposed SSM series operator and parallel operator. Compared with conventional state space modelling method, internal structure and parameters are not required in modelling procedure.

ACKNOWLEDGEMENTS

This work was supported by the ForskEL and EUDP Project "Voltage Control and Protection for a Grid towards 100% Power Electronics and Cable Network (COPE)" (Project No.: 880063).

BIBLIOGRAPHY

[1] E. A. A. Coelho, P. C. Cortizo, and P. F. D. Garcia, "Small-signal stability for parallel-connected inverters in stand-alone AC supply systems," IEEE Trans. Ind. Appl., vol. 38, no. 2, pp. 533–542, Mar./Apr. 2002.

[2] Y. Wang, X. Wang, F. Blaabjerg, and Z. Chen, "Harmonic instability assessment using state-space modeling and participation analysis in inverter-fed power systems," IEEE Trans. Ind. Electron., vol. 64, no. 1, pp. 806-816, Jan. 2017.

[3] N. Pogaku, M. Prodanovic, and T. C. Green, "Modeling, analysis and testing of autonomous operation of an inverter-based microgrid," IEEE Trans. Power Electron., vol. 22, no. 2, pp. 613–625, Mar. 2007.

[4] Y. Wang, X. Wang, F. Blaabjerg, and Z. Chen, "Small-signal stability analysis of inverter-fed power systems using component connection method," IEEE Trans. Smart Grid, vol. 9, no. 5, pp. 5301-5310, Sept. 2018.

[5] Rygg A, Molinas M, "Apparent Impedance Analysis: A small-signal method for stability analysis of power electronic-based systems," IEEE J. Emerg. Sel. Top. Power Electron., vol. 5, no. 4, pp. 1474-1486, Dec. 2017.

[6] M. K. Bakhshizadeh, C. Yoon, J. Hjerrild, C. L. Bak, L. Kocewiak, F. Blaabjerg, and B. Hesselbaek, "The application of vector fitting to eigenvalue-based harmonic stability analysis," IEEE J. Emerg. Sel. Top. Power Electron., vol. 5, no. 4, pp. 1487–1498, Dec. 2017.

[7] W. Cao, Y. Ma, L. Yang, F. Wang, and L. M. Tolbert, "D–Q impedance based stability analysis and parameter design of three-phase inverter-based AC power systems," IEEE Trans. Ind. Electron., vol. 64, no. 7, pp. 6017– 6028, Jul. 2017.

[8] A. Rygg, M. Molinas, E. Unamuno, C. Zhang, and X. Cai, "A simple method for shifting local dq impedance models to a global reference frame for stability analysis," arXiv preprint arXiv:1706.08313.

[9] C. Zhang, M. Molinas, A. Rygg, X. Cai, "Impedance network of interconnected power electronics systems: impedance operator and stability criterion," arXiv preprint arXiv:1811.06329.

[10] H. Liu, X. Xie, and W. Liu, “An oscillatory stability criterion based on the unified dq-frame impedance network model for power systems with high-penetration renewables,” IEEE Trans. Power Syst., vol. 33, no. 3, pp. 3472–3485, May 2018.
[11] H. Liu and X. Xie, "Impedance network modeling and quantitative stability analysis of sub-/super-synchronous oscillations for large-scale wind power systems," IEEE Access, vol. 6, pp. 34431-34438, 2018.
[12] B. Gustavsen, “Improving the pole relocating properties of vector fitting,” IEEE Trans. Power Del., vol. 21, no. 3, pp. 1587–1592, Jul. 2006.
[13] The Vector Fitting. Accessed on Jan. 18, 2019. [Online]. Available: https://www.sintef.no/projectweb/vectfit/
[14] B. Wen, D. Boroyevich, R. Burgos, P. Mattavelli, and Z. Shen, “Analysis of D-Q small-signal impedance of grid-tied inverters,” IEEE Trans. Power Electron., vol. 31, no. 1, pp. 675–687, Jan. 2016.